



Treatment of dyeing wastewater using submerged membrane bioreactor

A.H. Konsowa*, M.G. Eloffy, Y.A. El-Taweel

*Chemical Engineering Department, Faculty of Engineering, Alexandria University, Alexandria 21544, Egypt
Tel. +20 3 546 8502; Fax: +20 3 592 1854; email: akonsowa@alex-eng.edu.eg*

Received 26 January 2012; Accepted 29 May 2012

ABSTRACT

This study was carried out to evaluate the efficiency of aerobic submerged hollow fiber membrane bioreactor (HFMBR) in the removal of direct fast red dye-CI 81 from textile wastewater. The effect of hydraulic retention time (HRT), initial dye concentration, and transmembrane pressure (TMP) on the performance of submerged HFMBR was studied. The removal rate of chemical oxygen demand was found to increase with the increasing of HRT and decrease with increasing initial dye concentration and TMP. The rate of dye removal was found to increase with increasing HRT and decrease with the increasing TMP. The optimum color removal was obtained at initial dye concentration of 150–200 ppm. A mass transfer model for the dye removal using submerged membrane bioreactor system was developed and verified. The results revealed that there is a remarkable agreement between the theoretical results and experimental results with a deviation of 14.83%. The membrane fouling was investigated using electron dispersive X-ray (EDX) and scanning electron microscope (SEM) and compared with the EDX and SEM of the original one. SEM images revealed that there are some geometrical changes that occur in the membrane pores with fouling, while EDX mapping showed that most of the foulants deposited on the inner surface of the fiber.

Keywords: MBR; Membrane fouling; Microfiltration; Mass transfer; Modeling

1. Introduction

Biological treatment is an important aspect of industrial and municipal wastewater treatment and reuse processes [1]. The activated sludge process is commonly used in biological wastewater treatment for the removal of organic compounds [2]. Conventional activated sludge processes usually consist of an aeration tank and a clarifier, the effluent quality from the clarifier is however susceptible to large fluctuations as a result of complications arising from abnormal

microbial activities, such as bulking and foaming, which occur in the aeration tank, and makes separation of sludge from treated water difficult [3]. Since the early 70s, membrane separation processes (microfiltration [MF] and ultra-filtration [UF]) have been developed to replace the clarifiers traditionally used in activated sludge treatment system [4–6]. The advantages offered by the membrane bioreactor (MBR) over conventional treatment have been reviewed [7–11]. They include reduced footprint and sludge production through maintaining a high biomass concentration in the biological reactor. The system is also capable of

*Corresponding author.

handling wide fluctuations in influent quality, and the effluent can be reused directly for nonpotable purposes because filtration efficiency is such that high quality product water is generated [12]. The two main MBR configurations involve either submerged membranes or external circulation (side stream), this article will focus on submerged hollow fiber MBR. Like most of the membrane filtration processes, membrane fouling and its control is a major issue for an economically feasible MBR system [13]. In addition to mixed liquor suspended solids (MLSS), soluble microbial product (SMP) is considered as major membrane foulant [14,15]. Membrane fouling is characterized in general as a reduction of permeate flux through the membrane, as a result of flow resistance due to pore blocking, concentration polarization, and cake formation [16,17]. The effect of each of these fouling mechanisms on flux decline depends on factors such as membrane pore size, solute loading and size distribution, membrane materials and operating conditions, etc.

The aim of this research is to study the performance of submerged MBR for the removal of direct red dye from textile effluent under different operating conditions and developing a model describing the dye mass transfer through the submerged MBR.

2. Materials and method

2.1. Sample collection

The sludge sample was obtained from the west wastewater treatment plant in the west of Alexandria, Egypt with initial mixed liquor suspended solid equal to 3,000 mg/l. A nutrient-sufficient synthetic wastewater containing dye (direct fast red dye with CI 81), Commercial name is ISMA 8B red dye, was obtained from the chemical and dyeing company at Kafr Aldwar region near Alexandria, Egypt (see Fig. 1).

An existing laboratory-scale SMBR system was modified. The laboratory-scale membrane unit was a bundle of microporous (0.4 μm) polyethylene hollow fibers obtained from Korea Membrane Separation Co. (see Table 1).

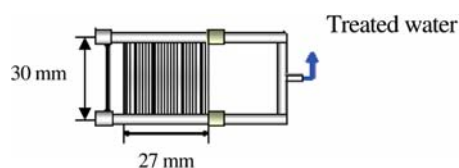


Fig. 1. The membrane unit.

Table 1
Characteristics of the membrane unit

| Category | Characteristics |
|-------------------|---|
| Product | MF membrane (Korea Membrane Separation, Co.) |
| Material | Polyethylene (PE) |
| Property | Hydrophilic |
| Nominal pore size | 0.4 μm |
| Out side diameter | 650 μm |
| In side diameter | 410 μm |
| Wall thickness | 120 μm |
| Module type | Hollow fiber |

2.2. Experimental set-up

The layout of the experimental setup is shown in Fig. 2. The submerged MBR system consists of mainly bioreactor tank 22 L volume (560 \times 110 \times 460 mm; $L \times W \times H$), permeate tank 6 L volume, and hollow fiber membrane bundle (Korea Membrane Separation Co.) with pore size 0.4 μm was immersed in the bioreactor tank, aeration system was developed using an air compressor 15 L/min air flow rate, and the permeate is filtrated under vacuum developed by a vacuum pump. Membrane was immersed vertically into the mixed liquor of the biological reactor, connected through the header system to the suction side. The membrane was subjected to a slight negative pressure. Water is drawn from the mixed liquor through the membrane wall surface into the capillary; the treated wastewater water was collected through the membrane discharge system. Air was pumped into the bottom of the bioreactor, developing a bubbly regime. The air stream performs the triple role of process, aeration, mixing of the biomass, and membrane cleaning. The used suction in this system eliminates the need to pump mixed liquor through the membrane system, significantly reducing the potential for membrane fouling and dramatically lowering energy consumption. Also, with the continuous movement of air bubbles around and through the fibers, a lowering concentration of biomass was maintained around the membrane, this minimizes the potential for membrane fouling.

2.3. Operating conditions

The temperature in the reactor was not controlled; however, the temperature was monitored regularly throughout the experiments. Values of pH were measured using a portable pH meter (JENWAY-370 pH Meter). Phosphate buffer solution was used to maintain pH at 7–8. The concentration of biomass in the

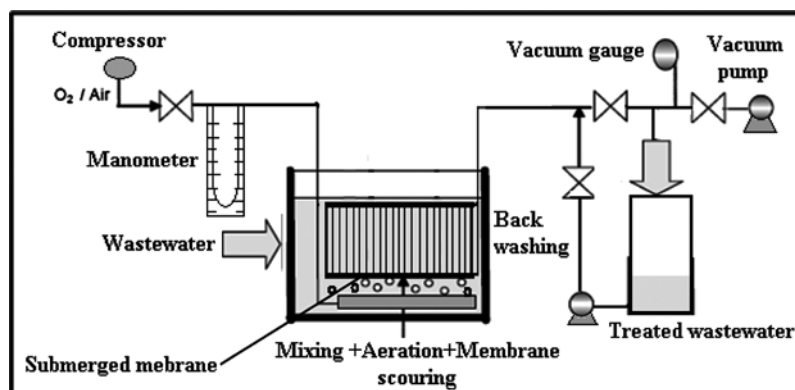


Fig. 2. Layout of the experimental setup.

aeration tank is represented by mixed liquor suspended solids (MLSS) mg/l; it ranged from 1,000 to 3,000 mg/l. Dissolved oxygen (DO) is required for the aerobic as well as the aerobic life forms, a minimum dissolved oxygen concentration of 2 mg/l throughout the aeration tank was to be maintained so as to prevent anaerobic conditions to prevail in the reactor (see Fig. 3). DO was determined using a portable DO meter (JENWAY-970 DO₂ Meter) to measure the DO in the aeration tank. During the experiments the food to micro-organism ratio F/M was maintained between 0.1 and 0.3.

2.4. Fouling analysis

To obtain information about the foulants remaining on the membrane, a module was autopsied. The fibers were removed and dried; in order to acquire images of both the inner side and the cross-section, a 45° angle cut was made between the cross-section and the bottom of the fibers. The samples were scanned

with a scanning electron microscope (SEM) (JSM 5300) equipped with energy dispersive X-ray analysis. EDX system was used to determine the morphology and chemical composition of the foulants on the membrane.

3. Results and discussion

3.1. Mixed liquor suspended solids

In the presence of nutrients (glucose, ammonium phosphate as source of necessary hydrocarbon), the micro-organism began to adapt with the dye and started to grow especially, when the concentration of dye increased and the biological degradation occurred. In this study, a reactor with sludge and a mode feeding strategy were explored for excess of sludge growth leading to increase in mixed liquor suspended solid (MLSS) concentration in direct contact with membrane and response of a part of fouling. So, washing between runs is necessary and chemical

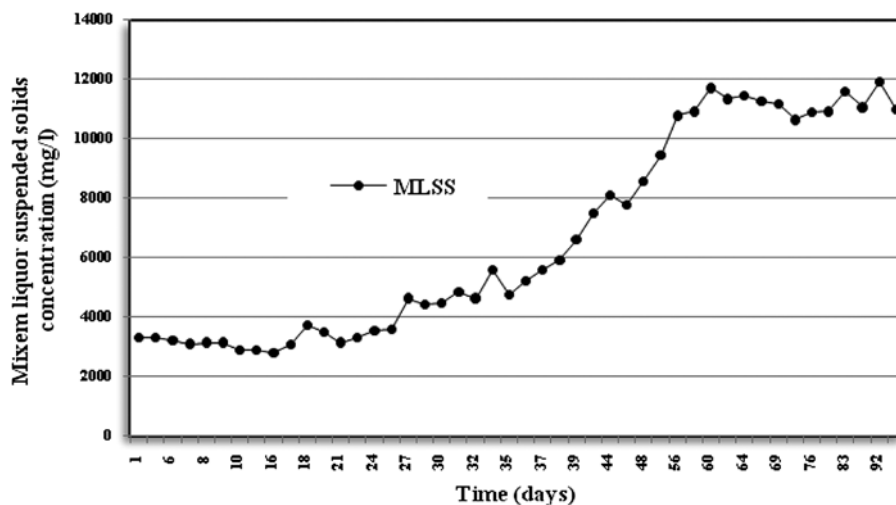


Fig. 3. Mixed liquor suspended solids concentrations during the experiments.

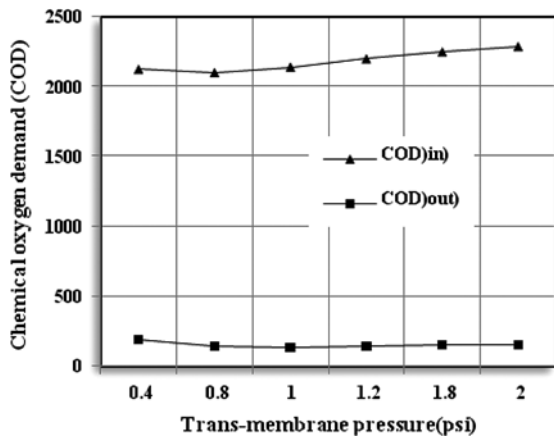


Fig. 4. The effect of TMP on the chemical oxygen demand.

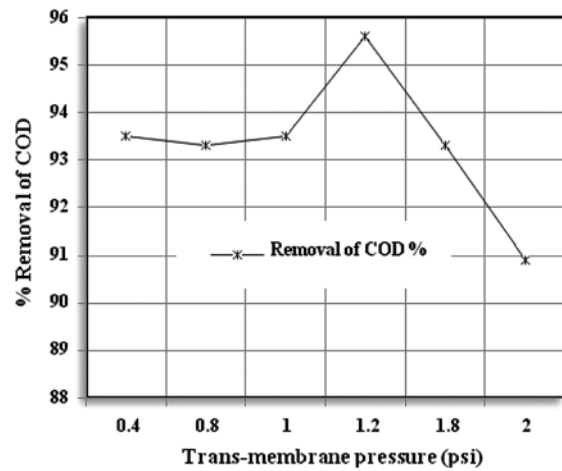


Fig. 7. The percentage removal of COD with different operating conditions.

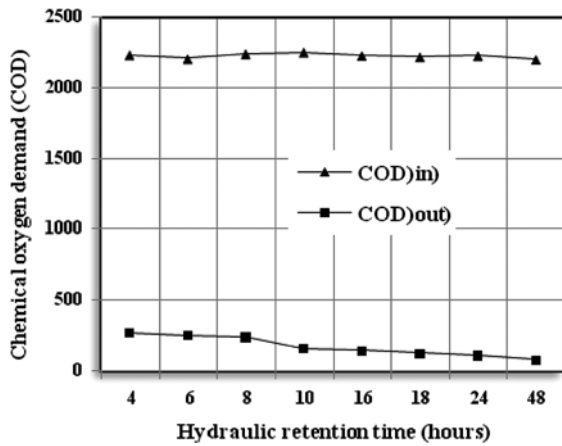


Fig. 5. The effect of HRT on the chemical oxygen demand.

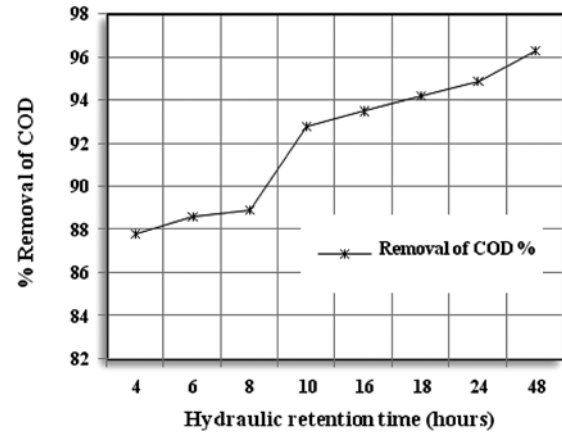


Fig. 8. The percentage removal of COD with different operating conditions.

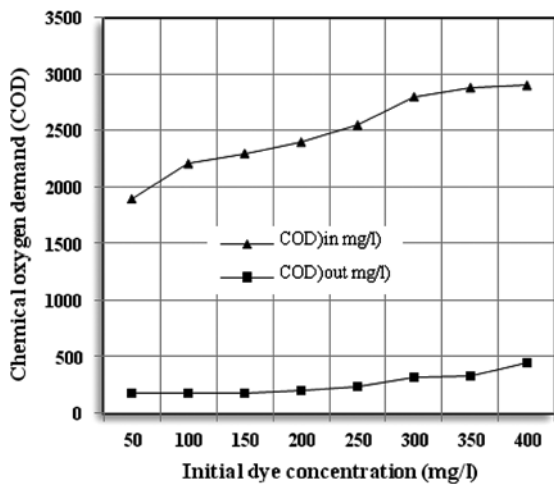


Fig. 6. The effect of initial dye concentration (C_0) on the chemical oxygen demand.

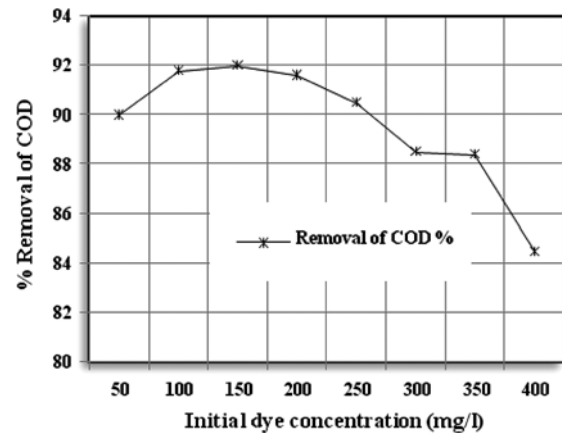


Fig. 9. The percentage removal of COD with different operating conditions.

cleaning should be carried out periodically using suitable chemical cleaning technique (sodium hypochlorite NaOCL is used in this case).

3.2. The removal of chemical oxygen demand

The influent wastewater chemical oxygen demand (COD) concentrations and effluent COD concentrations at different operating conditions were determined (see Figs. 4–9).

From the relation between the influent wastewater COD concentration and the effluent COD concentration at different operating conditions, it is clear that the increase in the operating pressure within the study range had a slight effect on the percentage removal of COD, the increase in the hydraulic retention time within the study range had a slight effect on the percentage removal of COD, and also the increase in the initial dye concentration within the study range had a significant effect on the percentage removal of COD.

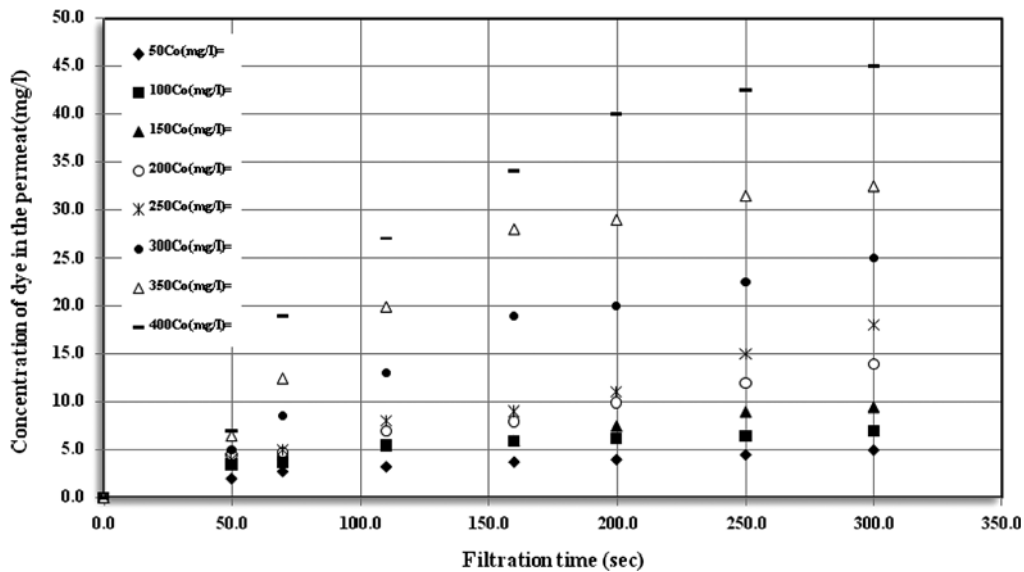


Fig. 10. The concentration of dye in the permeate with different C_0 .

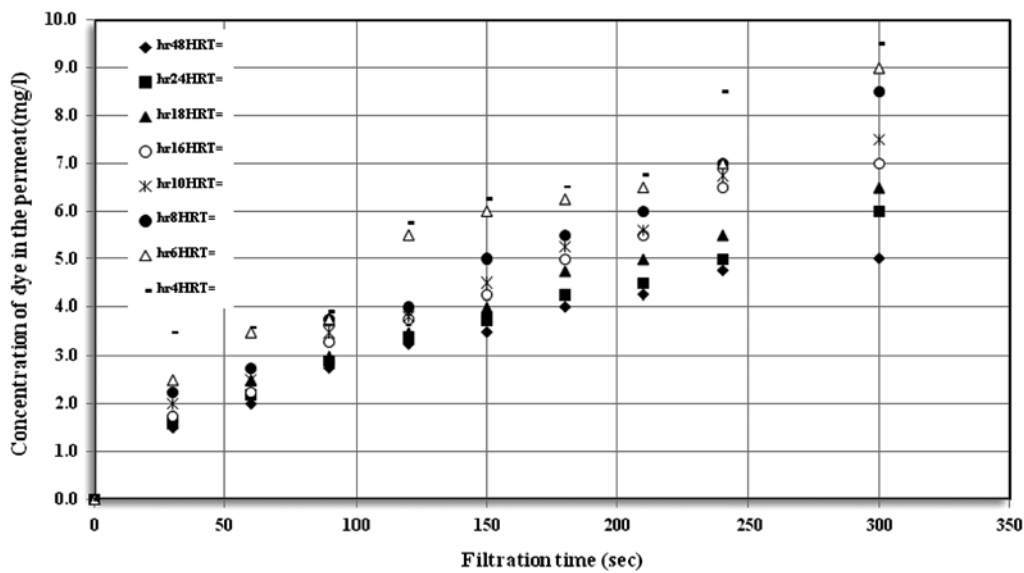


Fig. 11. The concentration of dye in the permeate with different HRTs.

3.3. The removal of dye

As shown in Figs. 10 and 11 the concentrations of treated wastewater for different initial dye concentrations (C_0) and different hydraulic retention times (HRTs) were observed and plotted against filtration time (see Figs. 12–14).

3.3.1. The effect of initial dye concentration (C_0)

The dye removal rate increases with increasing dye concentration up to initial dye concentration 150 mg/l and after this value the removal efficiency decreases. This may be explained in view of the biochemical reaction kinetics and the limited capacity of the dye bioremoval. In view of the narrow separation limitation of the membrane process, the micro-organism has the ability to biotreat the dye removal up to 150 ppm but after this concentration this ability was decreased drastically due to the limitation of the bioremoval mechanism. Removal rates would increase or

decrease depending on the surface area available for fouling formation treatment to occur.

3.3.2. The effect of hydraulic retention time

The percentage removal of dye increases with increasing the HRT and this could be explained in the view of low reactor performance which was observed at low HRTs. When there was insufficient contact time between the dye in feed and the micro-organism, minimal biological reactions occurred and low removal was observed. At 48hrs of HRT, 95% of removal was achieved.

3.4. The flux of permeate

The flux of permeate was followed with different runs for different operating conditions and the values of flux were plotted against these operating conditions (see Figs. 14–16).

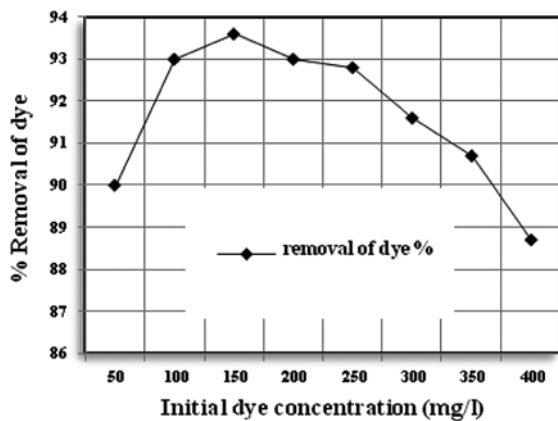


Fig. 12. Removal of dye at different C_0 .

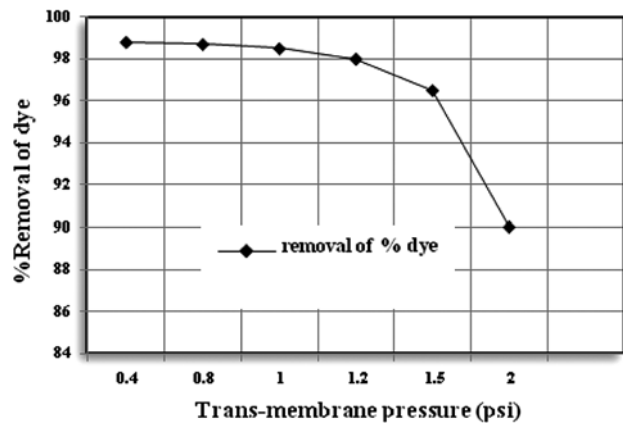


Fig. 14. Removal of dye at different TMP.

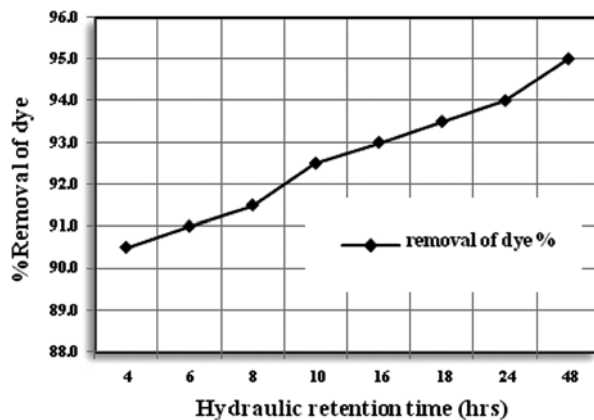


Fig. 13. Removal of dye at different HRTs.

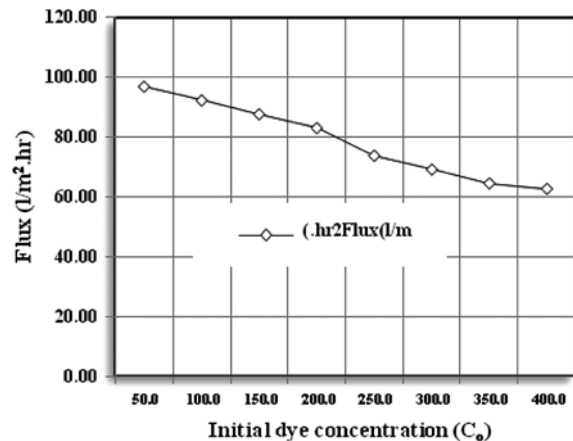


Fig. 15. The flux of permeate at different C_0 .

3.4.1. The effect of the transmembrane pressure (TMP)

From the experimental data, it was observed that a reduction in permeate flux with time was occurred and this is consistent with the previous studies [18,19]. As suspended solids accumulate near, on, and within the membrane lumen they may reduce the permeability of the membrane by blocking or constricting pores and forming a layer of additional resistance to flow across the membrane leading to reduction in permeate flux over time, which may be substantial and represented as a loss in the capacity of a membrane facility. Thus, reduction in permeate flux and procedures for maintaining permeate flux must be considered in both the design and operation of membrane facilities. The characteristics and location of the deposited materials can play an important role in determining the extent and reversibility of permeate flux

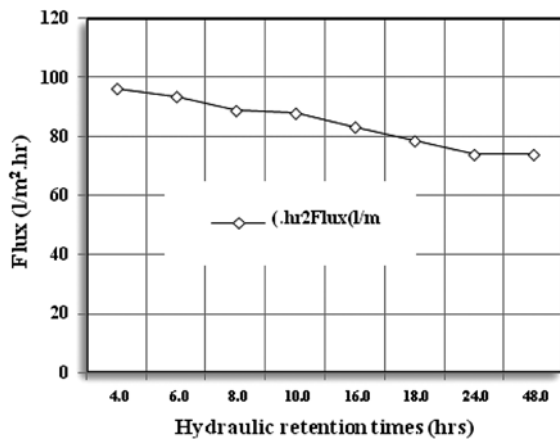


Fig. 16. The flux of permeate at different HRTs.

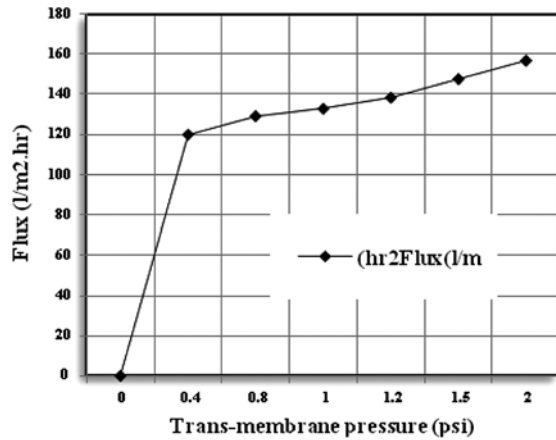


Fig. 17. The flux of permeate at TMP.

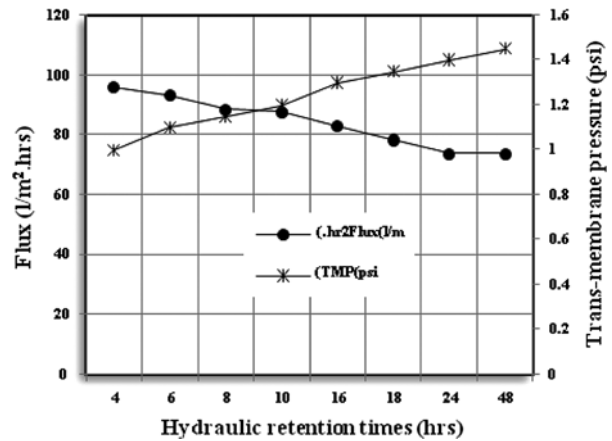


Fig. 18. Relation between TMP and flux with time.

decline. Washing the membrane, either hydraulically or chemically, may remove some of the accumulated materials and partially restore permeate flux. A reduction in permeate flux that cannot be reversed is referred to as membrane fouling. Frequently, both reversible and irreversible decreases in permeate flux decline are referred to as membrane fouling and materials in the water that produce reductions in permeate flux are collectively referred to as foulants (see Figs. 17 and 18).

3.5. Scanning electron microscopic

The SEM (JSM-5300) scanning electron micrograph images show the surfaces of clean membrane, and fouled membrane. New membrane surface is observed to be porous and free of particles (Fig. 19(A)–(C)). The surface of a fouled membrane shows the presence of a cake layer (Fig. 19(A)–(C')). The cake layer was non-porous in appearance, with rod-shaped bacteria and other materials. Surfaces were in general including foulants. The fouled membrane was fixed with a 0.5% sodium hypochlorite solution periodically. Membrane cleaning comprises of intermittent physical cleaning (usually back-washing) and periodic chemical cleaning. Chemical cleaning is expected to completely recover membrane flux, but produce toxic or contaminated wastewater because most cleaning agents are caustic and/or contain detergents and oxidizing agents as hypochlorite [18,20].

4. EDX—electron dispersive X-ray analysis

Surfaces of fouled membrane were analyzed with JSM 5300 electron dispersive X-ray detector (see Figs. 20 and 21).

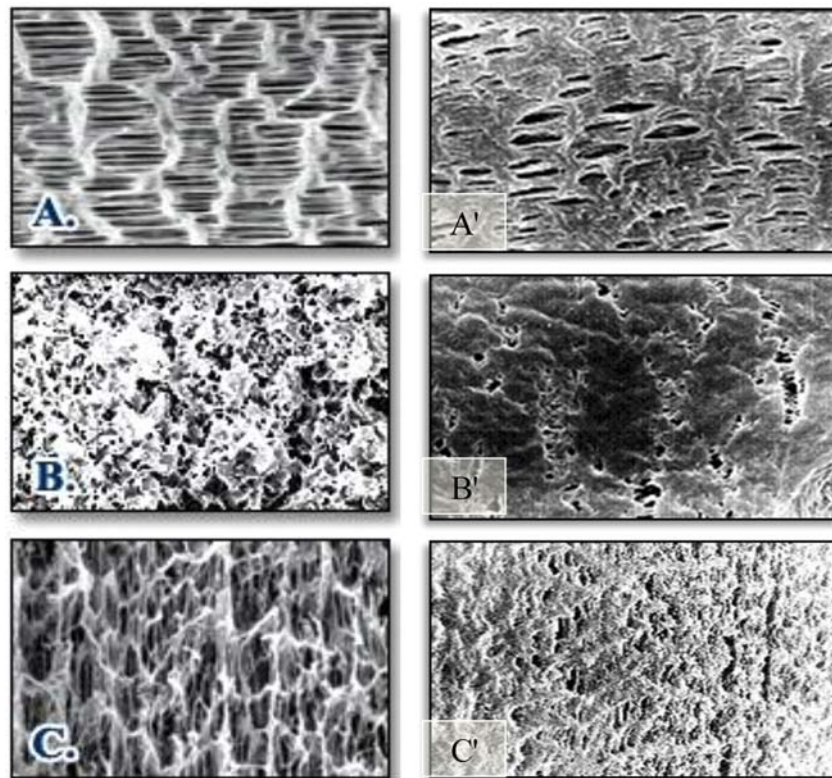


Fig. 19. Before fouling: (A) inner surface, (B) cross-section, and (C) longitudinal section. After fouling: (A) inner surface, (B) cross-section, and (C) longitudinal section.

4.1. Mass transfer model

4.1.1. Assumptions

The following assumptions are made in the estimation of mass transfer coefficients and additional assumption will be mentioned along with the development of the model:

- The reactor is completely mixed.
- The volume of the reactor is constant.
- Steady state operation.
- The membrane porosity = 50%.

A definition sketch of the MBR in Fig. 22 the effluent flux, J ($\text{g}/\text{m}^2\text{s}^1$), from the outside of the HFM (hollow fiber membrane) is described by:

$$J = K(C_b - C_t) \quad (1)$$

where K (m/s) is the overall mass transfer coefficient and C_b and C_t (g/m^3) are the bulk and out permeate dye concentration, respectively. At steady state, treated wastewater across membrane is described by:

$$v \frac{dC_b}{dx} = -Ka(C_b - c_t) \quad (2)$$

where v (m/s) is the velocity at the surface of membrane and a ($1/\text{m}$) is the membrane surface area per unit volume ($a=4/d$). Integration of Eq. (2) with the boundary condition $C_b=C_o$ at $X=0$ and $C_b=C_t$ at $X=\delta$, where δ is the wall thickness of the membrane fiber.

$$C_0 = (C_b - C_t) \exp\left(\frac{Ka\delta}{v}\right) + C_t \quad (3)$$

For the mass transfer tests, a completely mixed reservoir was connected to the outlet side of the membrane module. Due to the long residence time in the reservoir compared with the hollow fiber, a steady state assumption could be used. A mass balance on the membrane yields is shown in Fig. 23.

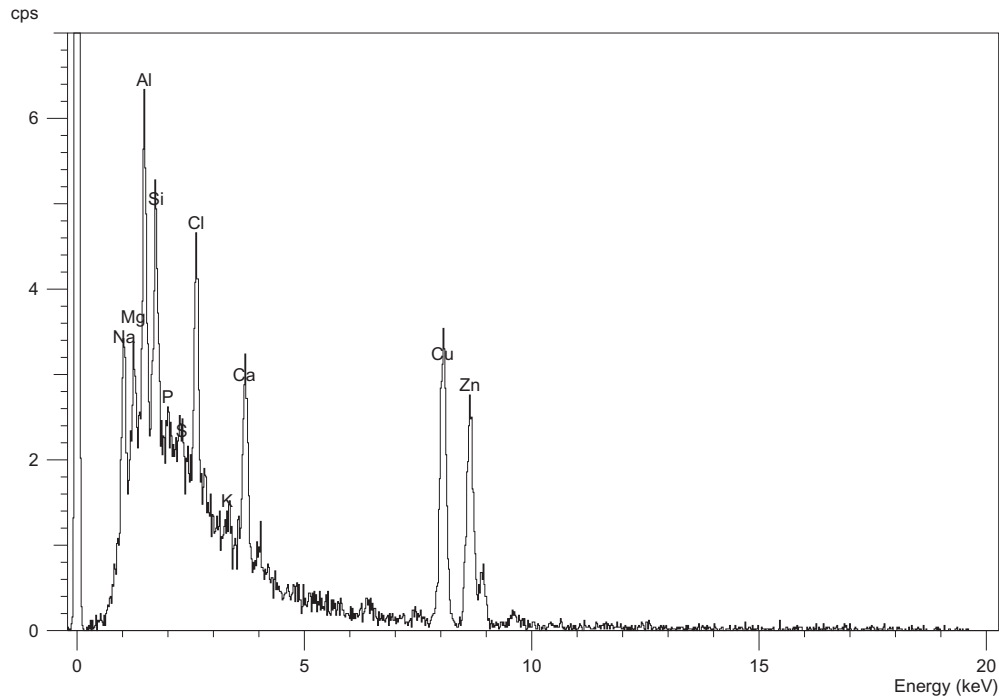
$$V \frac{dC_b}{dt} = Q(C_0 - C_t) \quad (4)$$

where V (m^3) is the volume of the bioreactor and Q (m^3/s) is the inlet flow rate.

Substitution of C_0 from Eq. (3) into Eq. (4) and integration with the boundary condition $C_b=0$ at time $t=0$ and $C_b=C_t$ at time $=t$ are given as follows:

EDX - Electron Dispersive X-ray Analysis:

Surfaces of fouled membrane were analyzed with JSM 5300 Electron Dispersive X-ray detector.



| Label | Range | Gross | Net | %total |
|-------|----------------|---------|---------|--------|
| N | 0.248 to 0.548 | 64.0 | 16.0 | 0.3 |
| Na | 0.887 to 1.188 | 1,663.0 | 319.0 | 5.7 |
| Mg | 1.207 to 1.308 | 853.0 | 103.0 | 1.8 |
| Al | 1.327 to 1.628 | 2,790.0 | 894.0 | 16.0 |
| Si | 1.648 to 1.888 | 2,229.0 | 585.0 | 10.5 |
| P | 1.908 to 2.168 | 1,589.0 | 49.0 | 0.9 |
| S | 2.188 to 2.467 | 1,611.0 | 74.0 | 1.3 |
| Cl | 2.487 to 2.767 | 2,034.0 | 827.0 | 14.8 |
| K | 3.168 to 3.467 | 925.0 | 149.0 | 2.7 |
| Ca | 3.547 to 3.848 | 1,459.0 | 603.0 | 10.8 |
| Cu | 7.907 to 8.208 | 1,437.0 | 1,109.0 | 19.9 |
| Zn | 8.488 to 8.788 | 1,177.0 | 849.0 | 15.2 |

Fig. 20. EDX analysis for outer surface of fouled membrane.

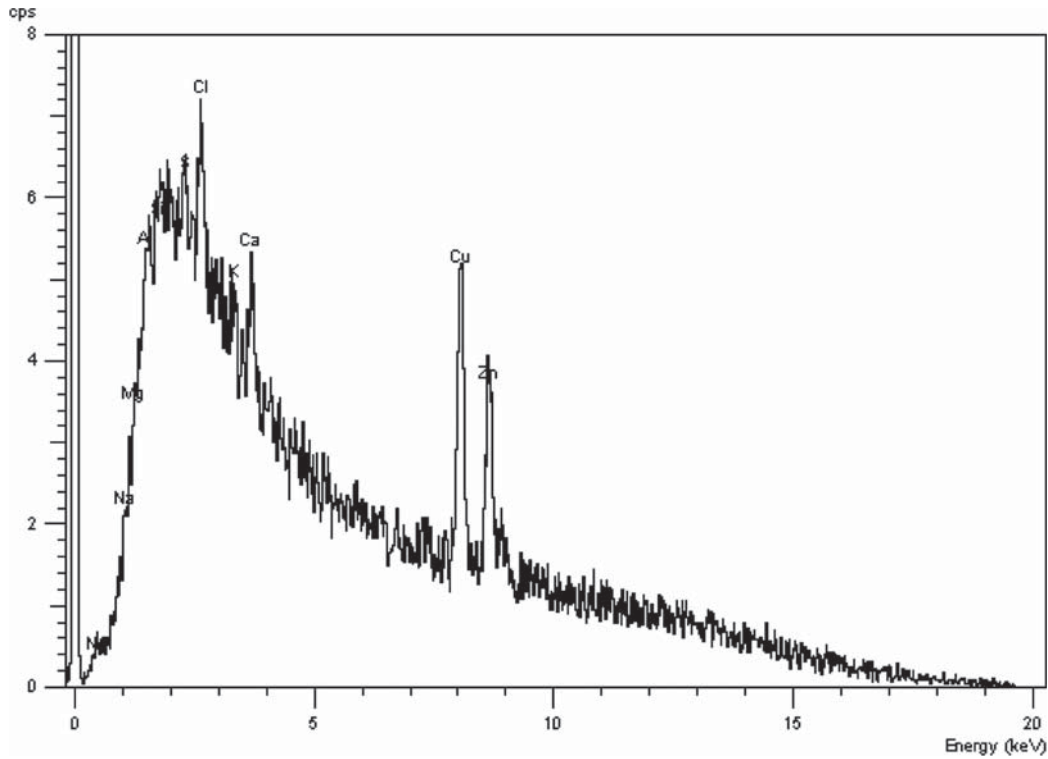
$$\ln\left(\frac{C_b}{C_b - C_t}\right) = \frac{Q}{V} \left[1 - \exp\left(\frac{Ka\delta}{v}\right) \right] \quad (5)$$

Experiments were conducted to determine the mass transfer coefficients at varying operating conditions. For each set of operating conditions, a steady inlet dye concentration 100 mg/l was applied to the submerged hollow fiber membrane and the bioreactor tank. Concentration of dye was measured over time. For each test, the data gave a linear relationship when

plotted in the form of Eq. (5). The theoretical overall mass transfer coefficient was calculated from the slopes.

4.2. Mass transfer experiments

Three main resistances may contribute to the overall resistance to mass transfer in the MBR: the membrane resistance k_m , the inside feed to the membrane



| Label | Range | Gross | Net | %total |
|-------|----------------|---------|---------|--------|
| N | 0.248 to 0.548 | 302.0 | 14.0 | 0.4 |
| Na | 0.887 to 1.188 | 1,567.0 | 31.0 | 1.0 |
| Mg | 1.207 to 1.308 | 1,028.0 | 53.0 | 1.6 |
| Al | 1.327 to 1.628 | 3,958.0 | 238.0 | 7.3 |
| Si | 1.648 to 1.888 | 3,846.0 | 258.0 | 8.0 |
| S | 2.188 to 2.467 | 4,447.0 | 127.0 | 3.9 |
| Cl | 2.487 to 2.767 | 4,478.0 | 226.0 | 7.0 |
| K | 3.168 to 3.467 | 3,525.0 | 109.0 | 3.4 |
| Ca | 3.547 to 3.848 | 3,434.0 | 330.0 | 10.2 |
| Cu | 7.907 to 8.208 | 2,752.0 | 1,192.0 | 36.8 |
| Zn | 8.488 to 8.788 | 2,201.0 | 665.0 | 20.5 |

Fig. 21. EDX analysis for inner surface of fouled membrane.

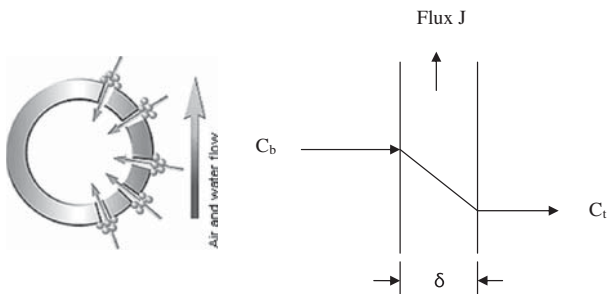


Fig. 22. Hollow fiber MBR (definition sketch used in mathematical model development).

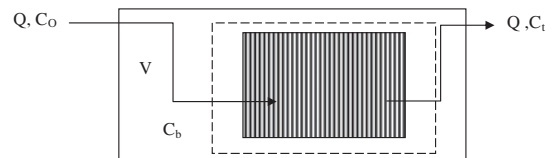


Fig. 23. Mass balance on the hollow fiber membrane tank.

resistance k_i , and the outside permeate resistance k_o . The overall resistance, K , is determined by the following equation:

$$\frac{1}{K} = \frac{1}{k_i} + \frac{1}{k_m} + \frac{1}{k_o} \quad (6)$$

A number of dimensionless correlation exist that can be used to predict the local mass transfer resistances based on the hydrodynamics of the system, the properties of the fluid and solute, and the system geometry.

For *laminar regime*, the Graetz–Leveque correlation can be used to estimate the mass transfer coefficient:

$$Sh = 1.86[Re^* Sc (d_h/L)]^{0.33} \quad (7)$$

where *Sh* is the Sherwood number ($Sh = kd/D$), *Re* is the Reynolds number ($Re = v de/\mu$), *Sc* is the Schmidt number ($Sc = \mu/\rho d$), and the effective diameter, *de* (m) used in the Reynolds number is the inner diameter of hollow fiber membrane. For *turbulent regime*, the Linton and Sherwood correlation can be used to estimate the mass transfer coefficient.

$$Sh = 0.023(Re)^{0.83}(Sc)^{0.33} \quad (8)$$

The mass transfer coefficient across a membrane is generally assumed to be that for mass transfer across a thin film [21].

$$K_m = \epsilon D/\delta \quad (9)$$

where ϵ is the membrane porosity and δ is the membrane wall thickness.

Overall mass transfer coefficient was calculated for the experimental conditions using Eqs. (6)–(9). Membrane properties (*d*, *d_{mv}* and *L*) were obtained from the membrane manufacturer. Diffusion coefficient of fluid across membrane is estimated using the fundamental of diffusion, where the basic flux across the membrane is exactly that for transport across a thin film Fick’s law.

$$j = D/\delta(C_b - C_t) \quad (10)$$

where *j* is the mass flux, *D* is the diffusion coefficient, δ is the membrane’s wall thickness, *C_b* is the concentration in the membrane on the feed side of the membrane, and *C_t* is the concentration within the membrane on the permeate side of the membrane [22]. A membrane porosity of 50% was assumed.

Hydrodynamics allow for understanding of the dynamic behavior of fluid flow through a bioreactor, affecting mass transfer of dye and overall reactor efficiency. In this study, the effect of hydrodynamics on removal efficiency was investigated. The HFMBR was

found to operate under various operating conditions [1]. The model is tested by comparing the experimental overall mass transfer coefficient which is generated by the model with the experimental overall mass transfer coefficient which is generated by actual experimental data of the submerged HFMBR. The results are compared at different operating conditions. As shown in Figs. 24–26, the results revealed that there is a remarkable agreement between the theoretical results and experimental results with deviation of about 8.6%.

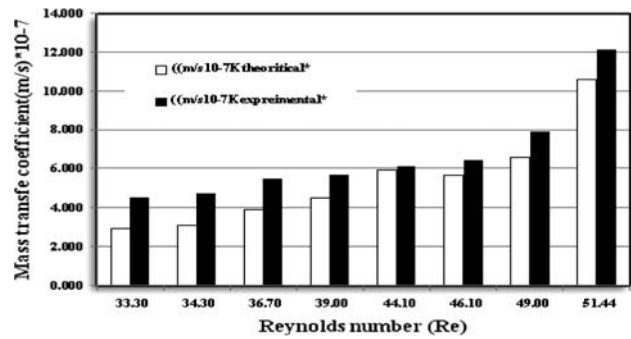


Fig. 24. Theoretical and experimental mass transfer coefficients for the MBR at different initial dye concentrations.

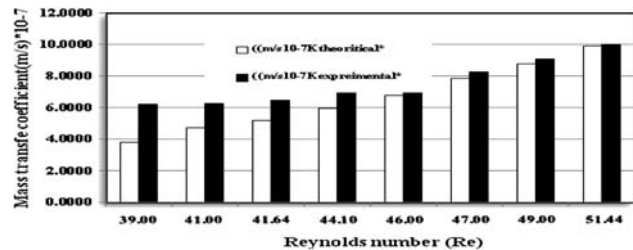


Fig. 25. Theoretical and experimental mass transfer coefficients for the MBR at different HRTs.

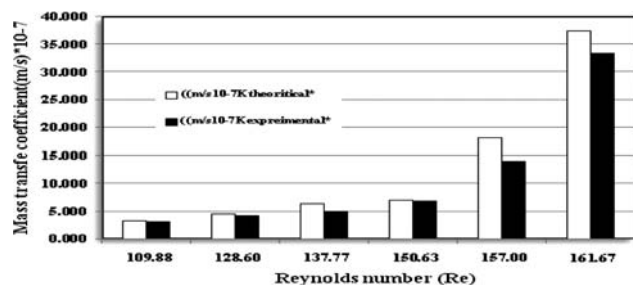


Fig. 26. Theoretical and experimental mass transfer coefficients for the MBR at different transmembrane pressures.

The following values were used in calculating the theoretical mass transfer coefficients using Eqs. (7)–(9): $d_h = 410 \mu\text{m}$, $\mu = 0.01 \text{ cm}^2 \text{ s}^{-1}$, $\rho = 1 \text{ g cm}^{-3}$, $\varepsilon = 0.5$, number of fibers = 1,050 module, and diameter = $650 \mu\text{m}$ $\delta = 120 \mu\text{m}$.

The model used for this study follows the model presented by [23].

5. Conclusion

Based on the results of this study, the following conclusions may be drawn:

- The submerged HFMBR proved to be an effective decolorization method with high removal efficiency and acceptable permeate flux. The submerged HFMBR is capable of achieving maximum removal of dye efficiency at low initial dye concentrations, high HRTs, and low operating pressure. Treatment efficiency of the submerged HFMBR process under different operating conditions was studied.
- The COD removal efficiency ranged from 87.7% to over 96.3%. The COD removal efficiency increased as hydraulic retention time increased. The COD removal efficiency ranged from 90.9% to over 95.6%. The COD removal efficiency increased as operating pressure decreased. The COD removal efficiency increased when the initial concentration of dye between 150 and 200 mg/l. After these values, the COD removal efficiency decreased with increasing the initial concentration of dye.
- The submerged HFMBR was considered to provide a significant mass transfer resistance; thus, the submerged HFMBR has been found to provide lower mass transfer in comparison to a membrane system for which the membrane resistance is taken into consideration due to cake formation and fouling.
- Surfaces of fouled membrane in this study were analyzed using a SEM (JSM-5300). SEM of membrane surface at the end of the experiment observed degrees of fouling. The fouled membrane is fixed with a 0.5% sodium hypochlorite solution periodically.

References

- [1] Metcalf & Eddy. Wastewater Engineering Treatment Disposal Reuse, 3d ed., McGraw Hill, New York, NY, 1991.
- [2] A.L. Lim, Renbi Bai, Membrane fouling and cleaning in microfiltration of activated sludge wastewater, *J. Membr. Sci.* 216(1–2) (2003) 279–290.
- [3] N.F. Gray, *Biology of Wastewater Treatment*, Oxford University Press, New York, NY, pp. 374–396 1989.
- [4] J. Arevalo, B. Moreno, J. Perez, M.A. Gomez, Applicability of the sludge biotic index (SBI) for MBR activated sludge control, *J. Hazard. Mater.* 167(1–3) (2009) 784–789.
- [5] S.P. Hong, T.H. Bae, T.M. Tak, S. Hong, A. Randall, Fouling control in activated sludge submerged hollow fiber membrane bioreactor, *Desalination* 143(3) (2002) 219–228.
- [6] B. Zhang, B. Sun, M. Ji, H. Liu, Population dynamics succession and quantification of ammonia-oxidizing bacteria in a membrane bioreactor treating municipal wastewater, *J. Hazard. Mater.* 165(1–3) (2009) 796–803.
- [7] T. Stephenson, S. Judd, B. Jefferson, J. Manem, Hydrodynamic control of bio-particle deposition in a MBR applied to wastewater treatment, *J. Membr. Sci.* 147 (1998) 1–12.
- [8] A.N.L. Ng, A.S. Kim, A mini review of modeling studies on membrane bioreactor (MBR) treatment for municipal wastewater, *Desalination* 212(1–3) (2007) 261–281.
- [9] Z. Wang, Z. Wu, Distribution and transformation of molecular weight of organic matters in membrane bioreactor and conventional activated sludge process, *Chem. Eng. J.* 150(2–3) (2009) 396–402.
- [10] J. Arevalo, G. Garralon, F. Plaza, B. Moreno, J. Perez, M.A. Gomes, Wastewater reuse after treatment by tertiary ultrafiltration and a membrane bioreactor (MBR): a comparative study, *Desalination* 243(1–3) (2009) 32–41.
- [11] M. Bernhard, J. Muller, T.P. Knepper, Biodegradation of persistent polar pollutants in wastewater: comparison of an optimized lab-scale membrane bioreactor and activated sludge treatment, *Water Res.* 40(18) (2006) 3419–3428.
- [12] C. Chiemchaisri, K. Yamamoto, S. Vigneswaran, House hold membrane bioreactor in domestic wastewater treatment, *Water Sci. Technol.* 27 (1993) 171–178.
- [13] W.J. Davies, M.S. Le, C.R. Heath, Intensified activated sludge process with submerged membrane microfiltration, *Water Sci. Technol.* 38(4–5) (1998) 421–428.
- [14] H. Nagaoka, S. Ueda, A. Miya, Influence of bacterial extracellular polymers on membrane separation activated sludge process, *Water Sci. Technol.* 34(9) (1996) 165–172.
- [15] I.S. Chang, C.H. Lee, Membrane filtration characteristics in membrane-coupled activated sludge system—the effect of physiological states of activated sludge on membrane fouling, *Desalination* 120 (1998) 221–233.
- [16] R.B. Bai, H.F. Leow, Microfiltration of activated sludge wastewater—the effect of system operation parameters, *Sep. Purif. Technol.* 29(2) (2002) 189–198.
- [17] R.B. Bai, H.L. Leow, Mufiltration of polydispersed suspension by a membrane screen/hollow fiber composite module, *Desalination* 140(3) (2001) 277–287.
- [18] X. Zhang, Y. Chen, A.H. Konsowa, X. Zhu, J.C. Crittenden, Evaluation of an innovative polyvinyl chloride (PVC) ultrafiltration membrane for wastewater treatment, *Sep. Purif. Technol.* 70(1) (2009) 71–78.
- [19] P.L. Clech, B. Jefferson, I.S. Chang, S.J. Judd, Critical flux determination by the flux-step method in a submerged membrane bioreactor, *J. Membr. Sci.* 227(1–2) (2003) 81–93.
- [20] J.S. Baker, L.Y. Dudley, Biofouling in membrane systems, *Desalination* 118(1–3) (1998) 81–90.
- [21] N. Cicek, M. Suidan, V. Urbin, J. Manem, Characterization and comparison of a membrane bioreactor in the treatment of wastewater containing high molecular weight compounds, *Water Environ. Res.* 71 (2000) 64–70.
- [22] E.L. Cussler, *Diffusion: Mass Transfer in Fluid Systems*, 2nd ed., Cambridge Press, Cambridge, 2003.
- [23] S.J. Ergas, D.E. Rheiheimer, Drinking water denitrification using a membrane bioreactor, *Water Res.* 38 (2004) 3225–3232.